

Influence of Carbon Group Substituents on Bond Shift and Electrochemical Reduction of Cyclooctatetraene

Stuart W. Staley,* Russell A. Grimm, and Rachel A. Sablosky

Contribution from the Department of Chemistry, Carnegie Mellon University, Pittsburgh, Pennsylvania 15213

Received September 25, 1996. Revised Manuscript Received December 23, 1997

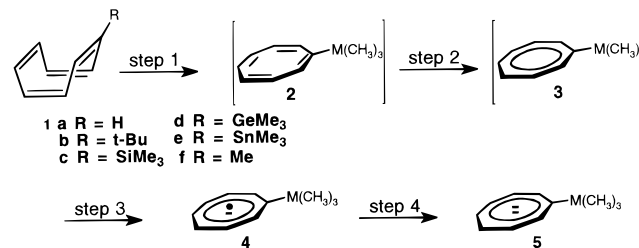
Abstract: The free energies of activation for bond shift in the carbon group substituted cyclooctatetraenes (COT–M(CH₃)₃) in THF-*d*₈ at 298 K have been determined to be 16.4, 16.2, 16.2, and 18.1 kcal/mol for M = Si, Ge, Sn, and C, respectively, and 15.6 kcal/mol for CH₃–COT. These data permit an interpretation of the previously reported opposite orders for the ease of the first and second electrochemical reductions in the Si, Ge, and Sn compounds. It is postulated that the order of the first reduction potential is controlled by a decrease in overlap between the substituent and the ring π orbitals in the order Si > Ge > Sn, whereas the second reduction potential is controlled by the energy gap between the symmetric π HOMO of the COT radical anion and an interacting substituent σ^* orbital of π symmetry ($\epsilon_{\sigma^*} - \epsilon_{\pi}$), which increases in the order Sn < Ge < Si. HF/3-21G molecular orbital calculations indicate that the high barrier for *t*-Bu–COT primarily reflects steric effects in the transition state.

Two decades ago Paquette and co-workers investigated the electrochemical reduction of cyclooctatetraene (COT) (**1a**) and its *tert*-butyl, trimethylsilyl, trimethylgermyl, trimethylstannyl, and methyl derivatives (**1b–f**, respectively) in hexamethylphosphoramide. The *tert*-butyl derivative was found to be the most difficult to reduce (most negative half-wave potential) to both the radical anion ($E_{1/2}^1$) and the dianion ($E_{1/2}^2$). Curiously, one-electron reduction of the heavier carbon group substituents (**1c–e**) becomes more difficult in the order Si < Ge < Sn whereas the order for the second reduction is reversed (Sn < Ge < Si). In every case the first reduction is more difficult than for unsubstituted cyclooctatetraene, but with the exception of **1b**, the second reduction is easier.

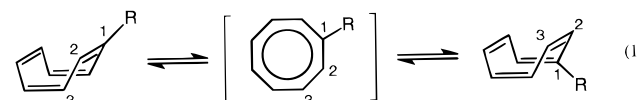
Paquette and co-workers did not address the reversed orders for the first and second reduction potentials of **1c–e** explicitly, but noted that the $E_{1/2}^1 - E_{1/2}^2$ gap was well correlated with the covalent radii of M = Si, Ge, and Sn and suggested that this has its origin in $C_{\pi} \rightarrow M$ resonance involving the d orbitals of M. It was assumed that steric effects on ring flattening were likely to have a much smaller differential effect than polar or resonance effects.¹

The reversed orders of $E_{1/2}^1$ and $E_{1/2}^2$ cannot easily be compared because the first reduction involves flattening the eight-membered ring in addition to electron transfer whereas transfer of the second electron takes place to an already planar radical anion. To make this comparison for **1b–e** without the complication of ring flattening, we have determined the energetics of the latter process separately. As shown in Scheme 1, this could, in principle, be accomplished by determining the kinetics of either ring inversion (**1** \rightarrow **2**) or of bond shift (**1** \rightarrow **3**). Ab initio molecular orbital calculations for the transition states and anions of COT (**2a**,² **3a**,^{2a} **4a**,^{2b,3} and **5a**,^{2b}) as well as spectroscopic studies (**2a**,⁴ **3a**,⁴ and **4a**,⁵) and single-crystal X-ray diffraction studies of **5a**,⁶ indicate that each of these geometries is planar. Since ring inversion in **1a–f** is not directly

Scheme 1



experimentally accessible by NMR spectroscopy, we have chosen to investigate the bond shift process (eq 1).



Experimental Section

Materials. Cyclooctatetraenes **1b**,⁷ **1c**,⁸ **1d**,⁸ **1e**,⁸ and **1f**¹ were synthesized by literature procedures. ¹³C NMR spectra (THF-*d*₈, 20 °C, 75 MHz) are as follows: **1b** δ 153.1, 133.5, 133.1, 132.2, 132.1,

(2) (a) Hrovat, D. A.; Borden, W. T. *J. Am. Chem. Soc.* **1992**, *114*, 5879. (b) Trindle, C.; Wolfskill, T. *J. Org. Chem.* **1991**, *56*, 5426. (c) Politzer, P.; Murray, J. S.; Seminario, J. M. *Int. J. Quantum Chem.* **1994**, *50*, 273. (d) Karadakov, P. B.; Gerratt, J.; Cooper, D. L.; Raimondi, M. *J. Phys. Chem.* **1995**, *99*, 10186.

(3) Hammons, J. H.; Hrovat, D. A.; Borden, W. T. *J. Am. Chem. Soc.* **1991**, *113*, 4500.

(4) Wenthold, P. G.; Hrovat, D. A.; Borden, W. T.; Lineberger, W. C. *Science* **1996**, *272*, 1456.

(5) Samet, C.; Rose, J. L.; Piepho, S. B.; Laurito, J.; Andrews, L.; Schatz, P. N. *J. Am. Chem. Soc.* **1994**, *116*, 11109; **1995**, *117*, 9381 and references cited.

(6) (a) Noordik, J. H.; van den Hark, T. E. M.; Mooij, J. J.; Klaassen, A. A. K. *Acta Crystallogr.* **1974**, *B30*, 833. (b) Noordik, J. H.; Degens, H. M. L.; Mooij, J. J. *Acta Crystallogr.* **1975**, *B31*, 2144. (c) Hu, N.; Gong, L.; Jin, Z.; Chen, W. *J. Organomet. Chem.* **1988**, *352*, 61.

(7) Miller, J. T.; DeKock, C. W.; Brault, M. A. *J. Org. Chem.* **1979**, *44*, 3508.

(8) Cooke, M.; Russ, C. R.; Stone, F. G. A. *J. Chem. Soc., Dalton Trans.* **1975**, 256.

(1) Paquette, L. A.; Wright, C. D., III; Traynor, S. G.; Taggart, D. L.; Ewing, G. D. *Tetrahedron* **1976**, *32*, 1885.

Table 1. Kinetic Data for Bond Shift in Carbon Group Substituted Cyclooctatetraenes

cmpd	substituent	temp range (K) ^a	$k_{bs}(298\text{ K})^b$	$\Delta G_{bs}^\ddagger(298\text{ K})^c$
1b	C(CH ₃) ₃	318–364	0.33	18.1
1c	Si(CH ₃) ₃	287–328	5.7	16.4
1d	Ge(CH ₃) ₃	280–320	9.2	16.2
1e	Sn(CH ₃) ₃	282–323	8.3	16.2
1f	CH ₃	272–311	22.9	15.6
1a	H	248–443		13.3 ^d

^a ± 1 K. ^b In s⁻¹; ± 20%. ^c ± 0.1 kcal/mol. ^d Calculated from data in ref 16. The rate constant was corrected to the unidirectional value, as discussed in ref 17.

131.7, 130.8, 123.6, 36.7 (C(CH₃)₃), 30.0; **1c** δ 149.9, 139.4, 135.4, 134.0, 132.6, 132.1, 132.0, 129.8, -1.6; **1d** δ 150.9, 137.2, 135.6, 134.0, 132.5, 132.3, 132.0, 129.3, -2.2; **1e** δ 152.0, 139.9, 137.6, 134.4, 132.5, 132.3, 132.0, 127.5, -9.8; **1f** δ 140.6, 135.7, 133.1, 132.7, 132.4, 131.5, 130.8, 127.4, 23.8. The italicized values are those for C₂–C₄ and C₆–C₈, which undergo exchange during bond shift. The signals for CH₃ and C₁ are the most upfield and downfield, respectively, in each case whereas the remaining signal is that for C₅.

NMR Measurements. NMR samples were prepared by dissolving ca. 0.2 mmol of cyclooctatetraene derivative and 10 μL of cyclohexane in 0.75 mL of THF-*d*₈. The sample was degassed with six freeze–pump–thaw cycles and sealed under vacuum. Temperatures above and below 313 K were calibrated with an ethylene glycol⁹ and a methanol¹⁰ chemical shift thermometer, respectively, and are reliable to ± 1 °C.

The rate constants for bond shift (k_{bs}) in **1b**–**f** were determined by measurement of the line widths of the ¹³C signals that undergo pairwise exchange (C₂ and C₈, C₃ and C₇, C₄ and C₆) and of cyclohexane, which served as an internal standard.¹¹ Measurements were made over ranges of ca. 40° after the onset of line broadening at temperatures just above the low-temperature region. Rate constants, averaged for at least two samples and extrapolated to 298 K by plotting ln(k/T) vs 1/ T , are reported in Table 1 along with the corresponding values of ΔG_{bs}^\ddagger calculated from the Eyring equation.

Computational Methods. Ab initio optimized geometries were calculated with the GAUSSIAN 92 series of programs¹² at the Hartree–Fock (HF) level of theory with 3-21G¹³ and 6-31G*¹⁴ basis sets. Optimized ground states and ring inversion transition states were shown to have zero and one imaginary frequency, respectively, by harmonic frequency analysis. Atomic charges were calculated by a natural population analysis (NPA).¹⁵

Results and Discussion

Bond Shift. Rate constants and free energies of activation for bond shift (ΔG_{bs}^\ddagger) in **1a**–**f** are reported in Table 1. To assess the significance of the ΔG_{bs}^\ddagger values in Table 1, we performed HF/3-21G geometry optimizations and harmonic frequency analyses on **1a**–**i**, as well as on the corresponding structures of **2** (Table 2). The ring inversion transition state

Table 2. Calculated Energy of the Ring Inversion Transition State Relative to the Ground State for Carbon Group Substituted Cyclooctatetraenes

cmpd	substituent	ΔE_{ri} (kcal/mol)		
		HF/ 3-21G	HF/ 3-21G + ZPE	HF/ 6-31G* + ZPE
1a	H	15.9	16.7	13.9
1b	C(CH ₃) ₃	20.6	21.6	
1c	Si(CH ₃) ₃	19.1	20.0	
1d	Ge(CH ₃) ₃	18.1		
1e	Sn(CH ₃) ₃	19.6		
1f	CH ₃	17.6	18.5	15.7
1g	SiH ₃	19.1	19.9	16.6
1h	GeH ₃	18.2	19.2	
1i	SnH ₃	19.8	20.6	

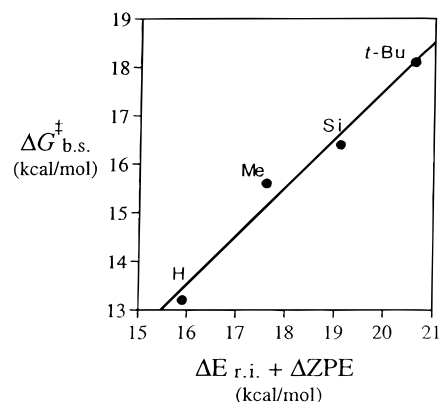


Figure 1. $\Delta G_{bs}^\ddagger(298\text{ K})$ vs the relative ground state and transition state energies for ring inversion ($\Delta E_{ri} + \Delta ZPE$) calculated at the HF/3-21G level for COT and carbon group substituted COTs (Si = Si(CH₃)₃).

(**2**) is a good model for the steric interactions in the bond shift transition state (**3**), which we were unable to calculate because of the size of the molecules and the multiconfiguration wave function required.^{2a,d} The validity of this model is supported by the excellent correlation ($r^2 = 0.979$) between ΔG_{bs}^\ddagger and the energy difference between the ground state and the transition state for ring inversion corrected for zero point energies ($(\Delta E + \Delta ZPE)_{ri}$) displayed in Figure 1.

We have shown recently in a study of monohalocyclooctatetraenes that both steric effects and the electronegativity of the substituent at C₁ influence the energy required for ring flattening.¹⁸ Steric effects result primarily from eclipsing of the substituent and the vicinal C₈–H₈ bond as the MC₁C₈H₈ dihedral angle is decreased from about 45° in the tublike ground state to 0° in the transition state, as well as from the interaction of the M(CH₃)₃ group with the vicinal C–H groups as $\angle C_2C_1C_8$ increases from ca. 123° in the ground state to 129–135° in the ring inversion transition state. They include both van der Waals interactions between proximate atoms and dipolar interactions of the C₁–substituent bond with the vicinal C–H bonds.

Electronegativity (hybridization) effects result from a difference in demand for C₁ s character in the bond with the substituent relative to that with a hydrogen atom in unsubstituted COT.^{19,20} It has been found by electron diffraction, for example, that $\angle C_2C_1C_6$ in para-substituted benzenes varies from 115.7

(16) Naor, R.; Luz, Z. *J. Chem. Phys.* **1982**, *76*, 5662.

(17) Goldman, G. D.; Roberts, B. E.; Cohen, T. D.; Lemal, D. M. *J. Org. Chem.* **1994**, *59*, 7421.

(18) Staley, S. W.; Grimm, R. A.; Martin, G. S.; Sablosky, R. A. *Tetrahedron* **1997**, *53*, 10093.

(19) Walsh, A. D. *Discuss. Faraday Soc.* **1947**, *2*, 18.

(20) Bent, H. A. *Chem. Rev.* **1961**, *61*, 275.

(9) Van Geet, A. L. *Anal. Chem.* **1968**, *40*, 2227.

(10) Van Geet, A. L. *Anal. Chem.* **1970**, *42*, 679.

(11) Sandström, J. *Dynamic NMR Spectroscopy*; Academic: New York, 1982; pp 14–18.

(12) Frisch, M. J.; Trucks, G. W.; Head-Gordon, M.; Gill, P. M. W.; Wong, M. W.; Foresman, J. B.; Johnson, B. G.; Schlegel, H. B.; Robb, M. A.; Replogle, E. S.; Gomperts, R.; Andres, J. L.; Raghavachari, K.; Binkley, J. S.; Gonzalez, C.; Martin, R. L.; Fox, D. J.; DeFrees, D. J.; Baker, J.; Stewart, J. J. P.; Pople, J. A. *GAUSSIAN 92, Revision A*; Gaussian, Inc.: Pittsburgh, PA, 1992.

(13) (a) Binkley, J. S.; Pople, J. A.; Hehre, W. F. *J. Am. Chem. Soc.* **1980**, *102*, 939. (b) Gordon, M. S.; Binkley, J. S.; Pople, J. A.; Pietro, W. J.; Hehre, W. J. *J. Am. Chem. Soc.* **1982**, *104*, 2797.

(14) (a) Hariharan, P. C.; Pople, J. A. *Chem. Phys. Lett.* **1972**, *16*, 217. (b) Francl, M. M.; Pietro, W. J.; Hehre, W. J.; Binkley, J. S.; Gordon, M. S.; DeFrees, D. J.; Pople, J. A. *J. Chem. Phys.* **1982**, *77*, 3654.

(15) (a) Reed, A. E.; Weinstock, R. B.; Weinhold, F. *J. Chem. Phys.* **1985**, *83*, 735. (b) Reed, A. E.; Weinhold, F. *J. Chem. Phys.* **1985**, *83*, 1736. (c) Reed, A. E.; Curtiss, L. A.; Weinhold, F. *Chem. Rev.* **1988**, *88*, 899.

Table 3. Calculated and Experimental Bond Angles at C₁ for Carbon Group Substituted Benzenes and Cyclooctatetraenes

cmpd	X	calcd $\angle C_2C_1C_8$ in COT-X ^{a,c}					
		exptl $\angle C_2C_1C_6$ ^{a,b}		HF/3-21G		HF/6-31G*	
		C ₆ H ₅ X	1,4-X ₂ C ₆ H ₄	GS ^d	TS ^e	GS ^d	TS ^e
1a	H	120.0	120.0	126.9	135.0	127.3	135.0
1b	C(CH ₃) ₃	117.1 ± 0.3 ^f		121.9	129.6		
1c	Si(CH ₃) ₃		115.7 ± 0.6	123.0	131.0		
1d	Ge(CH ₃) ₃			123.0	130.6		
1e	Sn(CH ₃) ₃			122.9	130.8		
1f	CH ₃	118.7 ± 0.4	117.1 ± 0.3	124.3	132.2	125.0	131.6
1g	SiH ₃	117.4		123.6	131.6	123.9	131.6
1h	GeH ₃			123.3	130.6		
1i	SnH ₃			123.2	131.1		

^a In degrees. ^b Electron diffraction values; from ref 21 unless indicated otherwise. ^c This work. ^d Ground state. ^e Ring inversion transition state. ^f Reference 23.

± 0.6° for *p*-trimethylsilyl substituents to 123.5 ± 0.1° for *p*-difluorobenzene.²¹ Thus, in this model electropositive substituents would be expected to be better accommodated in the ground state of COT than in the ring inversion or bond shift transition state where $\angle C_2C_1C_8$ increases by approximately 8°. Note that the same expectation is reached on the basis of a valence-shell electron-pair repulsion (VSEPR) model.^{21,22} Polarization of the C₁-Si bond toward the ring is postulated to increase the repulsion between the C-Si bond and the C₁-C₂ and C₁-C₈ bonds in COT. This causes these bonds to lengthen and $\angle C_2C_1C_8$ to decrease. The opposite changes occur for an electronegative substituent such as fluorine owing to polarization of the C-F bond away from C₁.

As shown in Table 3, the electron diffraction values of $\angle C_2C_1C_6$ in C₆H₅-R decrease in the order R = H > CH₃ > SiH₃ > *t*-Bu whereas the HF/3-21G values of $\angle C_2C_1C_8$ in COT-R decrease in the order H > CH₃ > SiH₃ > Si(CH₃)₃ > *t*-Bu. (The difference between CH₃ and SiH₃ disappears in the ring inversion transition state, but not in the ground state, of COT-R.) These orders are consistent with the hybridization and VSEPR models given above with the exception of the small values for *t*-Bu, which can be traced to steric effects that become more significant on going from the ground state to the transition state.

Additional support for this interpretation is given by the calculated bond lengths in Table 4. Thus, $r(C_1C_2)$ in COT-R increases in the order H < CH₃ < *t*-Bu < SiH₃ ≈ Si(CH₃)₃ in both the ground state and ring inversion transition state, a purely "hybridization" order, whereas $r(C_1C_8)$ increases in the order H < CH₃ < SiH₃ < Si(CH₃)₃ < *t*-Bu in both states. The position of *t*-Bu supports a strong steric contribution by this substituent.

Finally, $r(CR)$ increases by 0.0205 Å in the ground state of **1b** (R = *t*-Bu) relative to **1f** (R = CH₃), but this increase is 0.0292 Å for the more crowded transition state. The corresponding increases for **1c** (R = Si(CH₃)₃) relative to **1g** (R = SiH₃) are 0.0094 and 0.0110 Å for the ground and transition states, respectively. These values further support a strong steric contribution by *t*-Bu, but indicate only a small electronic and/or steric effect for Si(CH₃)₃ relative to SiH₃.

In summary, the order of ΔG_{bs}^\ddagger (H < CH₃ < Ge(CH₃)₃ ≈ Sn(CH₃)₃ ≈ Si(CH₃)₃ < *t*-Bu) can be understood as follows.

Table 4. Calculated Bond Lengths Involving C₁ for the Ground State (GS) and Ring Inversion Transition State (TS) of Carbon Group Substituted Cyclooctatetraenes

cmpd	substituent	calculation	$r(C_1C_2)$ ^a	$r(C_1C_8)$ ^a	$r(C_1M)$ ^{a,b}
1a	H	HF/3-21G	GS	1.320	1.477
			TS	1.323	1.477
		HF/6-31G*	GS	1.324	1.478
			TS	1.326	1.480
1b	C(CH ₃) ₃	HF/3-21G	GS	1.323	1.489
			TS	1.326	1.493
		HF/6-31G*	GS	1.326	1.486
			TS	1.330	1.491
1c	Si(CH ₃) ₃	HF/3-21G	GS	1.326	1.486
			TS	1.330	1.491
		HF/6-31G*	GS	1.324	1.481
			TS	1.327	1.486
1d	Ge(CH ₃) ₃	HF/3-21G	GS	1.324	1.481
			TS	1.327	1.486
		HF/6-31G*	GS	1.327	1.484
			TS	1.331	1.490
1e	Sn(CH ₃) ₃	HF/3-21G	GS	1.327	1.484
			TS	1.331	1.490
		HF/6-31G*	GS	1.326	1.485
			TS	1.329	1.491
1f	CH ₃	HF/3-21G	GS	1.321	1.484
			TS	1.325	1.489
		HF/6-31G*	GS	1.326	1.485
			TS	1.329	1.491
1g	SiH ₃	HF/3-21G	GS	1.326	1.485
			TS	1.330	1.489
		HF/6-31G*	GS	1.331	1.487
			TS	1.335	1.492
1h	GeH ₃	HF/3-21G	GS	1.323	1.479
			TS	1.327	1.483
		HF/6-31G*	GS	1.326	1.483
			TS	1.330	1.489
1i	SnH ₃	HF/3-21G	GS	1.326	1.483
			TS	1.330	1.489

^a In angstroms. ^b M is the substituent.

Each substituent increases ΔG_{bs}^\ddagger relative to unsubstituted COT due to a loss of s character in the exocyclic orbital of the substituted carbon on going from the ground state to the transition state, as reflected in increases of ca. 0.01 Å calculated for $r(CR)$ (R = CH₃, SiH₃, and Si(CH₃)₃). Compounds **1c–e** have essentially identical ΔG_{bs}^\ddagger values because the Pauling electronegativities (χ_P) of Si, Ge, and Sn are nearly identical (χ_P = 2.55, 1.92, 1.99 and 1.82 for C, Si, Ge and Sn, respectively).²⁴ In addition to electronegativity (hybridization or VSEPR) effects, the *t*-Bu group (**1b**) also exerts a significant steric retardation on bond shifting, resulting in an increase in ΔG_{bs}^\ddagger of 2.5 kcal/mol relative to methyl (**1f**). The assumption of Paquette et al.¹ that steric effects are comparable in **1c–e** is probably valid since our calculations show only small differences in the increase in $r(CR)$ between the ground state and transition state for SiH₃, GeH₃, and SnH₃ vs Si(CH₃)₃, Ge(CH₃)₃, and Sn(CH₃)₃, respectively.

Electrochemical Reduction. We now address the central issue of this paper, the opposite orders of difficulty of one-

(21) Domenicano, A. *Methods Stereochem. Anal.* **1988**, 10 (*Stereochem. Appl. Gas-Phase Electron Diff.*, Pt. B), 281.

(22) Gillespie, R. J. *Angew. Chem., Int. Ed. Engl.* **1967**, 6, 819; *J. Chem. Educ.* **1970**, 47, 18.

(23) Campanelli, A. R.; Ramondo, F.; Domenicano, A.; Hargittai, I. J. *Phys. Chem.* **1994**, 98, 11046.

(24) Shriver, D. F.; Atkins, P. W.; Langford, C. H. *Inorganic Chemistry*; Freeman: New York, 1990; pp 31–33, 640–1.

Table 5. Substituent Effects on Bond Shift and Electrochemical Reduction for Carbon Group Substituted Cyclooctatetraenes

cmpd	substituent	steps 1 + 2 ^a	step 3 ^a	step 4 ^a
		$\Delta\Delta G_{bs}^{\ddagger b}$	$\Delta E_{1/2}^1 - \Delta\Delta G_{bs}^{\ddagger c}$	$\Delta E_{1/2}^2 d$
1b	C(CH ₃) ₃	+4.8	+1.6	+1.7
1c	Si(CH ₃) ₃	+3.1	-2.3	-2.7
1d	Ge(CH ₃) ₃	+2.9	-1.9	-2.9
1e	Sn(CH ₃) ₃	+2.9	-1.0	-3.5
1f	CH ₃	+2.3	+0.6	+0.8

^a See Scheme 1 for definition of steps 1–4; positive and negative numbers signify greater and lesser energy requirements, respectively, relative to cyclooctatetraene. $E_{1/2}$ values are from ref 1. ^b $\Delta G_{bs}^{\ddagger}(\text{COT}-\text{M}(\text{CH}_3)_3) - \Delta G_{bs}^{\ddagger}(\text{COT})$; ± 0.2 kcal/mol. ^c $\Delta E_{1/2}^1 = E_{1/2}^1(\text{COT}) - E_{1/2}^1(\text{COT}-\text{M}(\text{CH}_3)_3)$; ± 0.3 kcal/mol. ^d $E_{1/2}^2(\text{COT}) - E_{1/2}^2(\text{COT}-\text{M}(\text{CH}_3)_3)$; ± 0.1 kcal/mol.

electron (Si < Ge < Sn) vs two-electron (Sn < Ge < Si) electrochemical reduction of **1c–e**. In Table 5 we present the substituent effect on the energetics of several of the steps in Scheme 1 by comparing substituted cyclooctatetraenes **1b–f** with the parent compound (**1a**). Bond shift (ΔG_{bs}^{\ddagger}) corresponds to the sum of steps 1 and 2 in Scheme 1, whereas reduction of **3** to **4** ($\Delta E_{1/2}^1 - \Delta\Delta G_{bs}^{\ddagger}$) and **4** to **5** ($\Delta E_{1/2}^2$) correspond to steps 3 and 4, respectively. (Two-electron reduction of cyclooctatetraene is given by the sum of steps 1–4.)

The two donor groups (methyl and *tert*-butyl) increase the energy for step 3 by about the same amount as that for step 4. In contrast, not only do the electron acceptors (Si(CH₃)₃, Ge(CH₃)₃, and Sn(CH₃)₃) decrease the energies of steps 3 and 4, but they decrease that of step 4 more in every case. Note that our bond shift data show that the opposite orders of the first and second reduction potentials for **1c–e** are maintained even after the energy of the ring flattening step is factored out of the first reduction potential.

Since the interaction between the highest symmetric COT π orbital (i.e., that with large coefficients on C₁, C₃, C₅, and C₇) and the lowest σ^* orbital of π symmetry on the substituent group (σ_{π}^*) is relatively small, we may estimate the interaction energy (E) between these orbitals by second-order perturbation theory (eq 2),

$$E = \frac{\langle \pi | H' | \sigma_{\pi}^* \rangle^2}{\epsilon_{\sigma_{\pi}^*} - \epsilon_{\pi}} \quad (2)$$

where H' is the interaction Hamiltonian and $\epsilon_{\sigma_{\pi}^*}$ and ϵ_{π} are the energies of the interacting σ_{π}^* and π orbitals, respectively. Because of the atomic radius of M and the concomitant increase in the C–M bond length, the overlap between π and σ_{π}^* (and therefore the square of the resonance integral ($\langle \pi | H' | \sigma_{\pi}^* \rangle^2$)) decreases in the order Si > Ge > Sn, while the energy gap

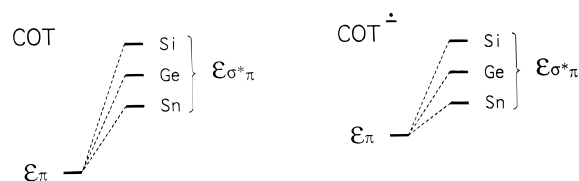


Figure 2. Interaction diagram showing the mixing of the lowest σ^* orbital of π symmetry (σ_{π}^*) on Si, Ge, or Sn with the symmetric π HOMO of COT (left) or the radical anion (right). Orbital energies are not to scale.

between these orbitals (as shown by electron transmission spectroscopy of (CH₃)₃MCl²⁵ and (CH₃)₄M,²⁶ which gives $\epsilon_{\sigma_{\pi}^*}$) decreases in the order Si > Ge > Sn. (The energetic effect of the donor groups (methyl and *tert*-butyl) is determined by σ_{π} -(substituent)- π^* (COT) interactions.)

The reversed trends in steps 3 and 4 can now be understood on the basis of the following model (see Figure 2). Since the π - σ_{π}^* energy gap is relatively large in the bond shift transition state (**3c–e**), the stabilization of step 3 relative to COT (Si > Ge > Sn; Table 5) is determined primarily by the C–M overlap, which is proportional to the numerator of eq 2 and decreases in the order Si > Ge > Sn.²⁷ On the other hand, ϵ_{π} is destabilized on reduction to the radical anion due to the addition of an extra electron to the π system, resulting in a decrease in $\epsilon_{\sigma_{\pi}^*} - \epsilon_{\pi}$. This, coupled with a relatively unchanged resonance integral, causes the relative stabilization of step 4 (Sn > Ge > Si) to be controlled by the denominator of eq 2. The energetics of the first and second reduction steps of **1c–e** relative to COT can be said to result from *overlap control* and *energy gap control*, respectively. We are currently attempting to assess the generality of this model.²⁸

Acknowledgment. We thank the National Science Foundation and the Carnegie Mellon SURG program for partial support of this research.

JA963359P

(25) Modelli, A.; Scagnolari, F.; Distefano, G.; Guerra, M.; Jones, D. *Chem. Phys.* **1990**, *145*, 89.

(26) Giordan, J. C.; Moore, J. H. *J. Am. Chem. Soc.* **1983**, *105*, 6541.

(27) The same order was found for the MCD *B* term of the L_b transition of M(CH₃)₃-substituted benzene and was attributed to a reduced π resonance integral in the order Si > Ge > Sn: Michl, J. *Tetrahedron* **1984**, *40*, 3845.

(28) This explanation may be oversimplified since it ignores a possible role for configuration interaction, vibronic coupling, and the Boltzmann effect. However, we believe that our model addresses the major elements of the substituent effect in these COTs. A reviewer has suggested that the presence of close-lying HOMOs and LUMOs of different symmetries in **1c–e** may be responsible for the order of $E_{1/2}^1$ if the singly occupied MO changes from antisymmetric to symmetric on going from **1c^{•-}** to **1e^{•-}**. However, even if an electron is added to an antisymmetric orbital, the delocalization onto the substituent of the π electrons in the corresponding symmetric orbital will increase due to the increase in its π orbital energy illustrated in Figure 2. It is this delocalization that is addressed by our model.